Max-Planck-Institut für Meteorologie

Report No. 10

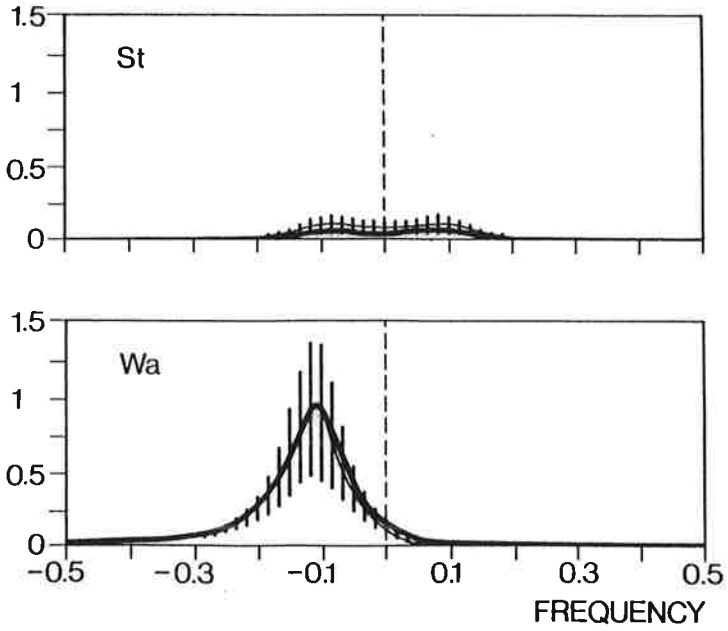

MONTE CARLO EXPERIMENTS WITH FREQUENCY-WAVENUMBER SPECTRA

by

UTE LUKSCH · HANS VON STORCH · YOSHIKAZU HAYASHI

HAMBURG, SEPTEMBER 1987

AUTHORS:

UTE LUKSCH — MAX-PLANCK-INSTITUT FÜR METEOROLOGIE

HANS VON STORCH — MAX-PLANCK-INSTITUT FÜR METEOROLOGIE

YOSHIKAZU HAYASHI — GFDL, PRINCETON UNIVERSITY
P.O. BOX 308
PRINCETON, NEW JERSEY 08542
USA

MAX-PLANCK-INSTITUT
FÜR METEOROLOGIE
BUNDESSTRASSE 55
D-2000 HAMBURG 13
F.R. GERMANY

Tel.: (040) 41 14 - 1
Telex: 211092
Telemail: K. Hasselmann
Telefax: (040)4114-298

Monte Carlo experiments with frequency-wavenumber spectra

Ute Luksch
Hans von Storch, Max-Planck-Institut für Meteorologie, Hamburg , FRG
Yoshikazu Hayashi, Geophysical Fluid Dynamics Laboratory, Princeton, USA

Abstract

We consider the ability of two-sided frequency wavenumber spectral analysis to infer the moving and standing wave variance from the spectral parameters of a bivariate, first order autoregressive process. This is done by applying the decomposition to known spectra and to spectra estimated from samples generated from processes with specified spectra. In particular, a series of Monte Carlo experiments is conducted with different sets of process parameters.

When the true spectra are known, the decomposition generally produces results which are easily interpreted in terms of standing and travelling waves. However, in the case of a damped, migrating, nonisotropically forced oscillation, the derived travelling wave variance is not necessarily non-negative. In this case the scheme's implicit assumption of statistical independence of standing and travelling waves is violated.

When the spectra are estimated from finite samples of time series, the results are less satisfactory. While the estimate of the frequency wavenumber spectrum appears fairly realistic, the separation into standing and travelling wave variance introduces systematic errors if the available data is limited. This is mainly due to the scheme's inability to identify a zero coherence.

1. Introduction

Space-time spectral analysis in meteorology was developed by Deland (1964) by relating the time quadrature spectrum of the zonal sine and cosine coefficient time series to the intensity of travelling waves. Kao (1968, 1970) estimated the space-time spectra by expanding the time series into a series of cosines and sines under the assumption of temporal periodicity. Since the latter assumption is not fulfilled in meteorological applications, Hayashi (1971, 1982) modified the procedure by taking into account the statistical characater of the time series.

The space-time spectral analysis is done in four steps, namely:

a) Expansion of global fields along latitudes into a finite series of trigonometric functions (i.e. Fourier analysis)
b) Spectral analysis of the resulting bivariate time series of sine and cosine coefficients.
c) Separation into east- and westward moving components.
d) Interpretation of the coherent part of the east- and westward moving components as a standing waveform. The remaining variance is attributed to travelling waves.

The spatial decomposition into zonal wavenumbers,step (a), is not critical, because it may be seen as a fully reversible coordinate transformation. The condition of periodicity is fulfilled; so the initial information may be precisely reconstructed from the Fourier coefficients.

In practice, the analysis of temporal behaviour, step b), is potentially misleading, since it is associated with the estimation of statistical parameters by means of a finite time series, which is known to be difficult (e.g Jenkins and Watts, 1968). The question is, to what extent the result of the analysis may be distorted by sample details, i.e. whether it is possible to extract reliable estimates of the true spectra.

The algorithm to split up the waves first into east- and westward moving components (step (c)) and secondly into standing and travelling parts (step (d)) has been derived from space-time series, which are periodic in space and time (Hayashi, 1971, 1973, 1977). Step (d) involves a working assumption that standing and travelling waves are incoherent, which is certainly fulfilled if they are of different origin or are far away from the same origin.Actual time series do

not fulfill the condition of (temporal) periodicity. Instead, they have to be seen as random realisations of bivariate stochastic processes. The question is, whether the concept may be used to interpret in a useful manner finite time series of Fourier coefficients generated by stochastic processes.

For this purpose, we study bivariate autoregressive processes of order one (Jenkins and Watts, 1968).

$$x_t = Ax_{t-1} + n_t \tag{1.1}$$

where $A = (a_{ij})$, $i,j = 1,2$ is a 2x2 matrix and $x_t = (C_t, S_t)$, $n_t = (z_t, z_t')$ are two-dimensional vectors. C_t and S_t may be identified with cosine and sine Fourier coefficients. The components of n_t are white noise with predetermined variances $\sigma^2_{z'}$ and σ^2_z. Their ratio is denoted by

$$b = \sigma^2_{z'} / \sigma^2_z \geq 0 \tag{1.2}$$

We assume that z_t and $z_{t'}$ are independent. This assumption is no limitation in our study. If this is not fulfilled, the 2-dimensional coordinates may be transformed such that in the new coordinate system the noise appears uncorrelated.

After presenting and briefly discussing the basic formulae proposed by Hayashi in Section 2, we calculate the 2x2 spectral matrix of the process (1.1) for a number of predetermined matrices A and ratios b and calculate the standing and travelling waveparts. Since matrix A and ratio b are known, the result can be considered with regard to the validity of the decomposition.

The estimation problem mentioned previously is considered in Section 3 of this paper. For this purpose random time series are generated by means of (1.1) with matrices A with predetermined values. Since the "true" wave decompositions are known from the analysis discussed in Section 2, one may assess the problems connected with the estimation of parameters by means of time series of finite length.

2. Known stochastic processes

A spatially periodic space time series h_{xt} ($0 \leq x \leq 2\pi$) may be expanded into a Fourier series in space:

$$h_{xt} = \sum_{m} H_{mt} e^{i m x} \qquad (2.1)$$

The spatial Fourier coefficients H_{mt} form a complex time series and may be represented by real coefficients:

$$H_{mt} = \frac{1}{2} (C_{mt} - i S_{mt}) \qquad (2.2)$$

In the following we consider only one spatial wavenumber m at a time. Therefore, we skip the index m in the formulae for the sake of clarity and convenience.

The frequency-wavenumber spectrum Γ_h is defined as (time) spectrum Γ_{HH} of the complex spatial Fourier coefficient H_t (Hayashi, 1982). In real quantities, it is expressed in terms of the power spectra Γ_{CC} and Γ_{SS} of the real spatial Fourier coefficients C and S and their quadrature-spectrum Q_{CS}:

$$\Gamma_h(f) = \Gamma_{HH}(f) = \frac{1}{4} \left\{ \Gamma_{CC}(f) + \Gamma_{SS}(f) - 2 Q_{CS}(f) \right\} \qquad (2.3)$$

The spectral densities at positive (negative) frequencies f are attributed to the variance of westward (eastward) moving components.

The standing part St is defined as that part of the east-and westward moving components which are coherent and of equal amplitude:

$$St(f) = 2 \cdot |\Gamma_{HH^*}(f)| = 2 [\Gamma_h(+f) \Gamma_h(-f)]^{1/2} Coh_{HH^*}(f) \qquad (2.4)$$

The coherence of the east- and westward moving components is measured by the coherence spectrum Coh_{HH^*} of the complex spatial Fourier coefficient H and its complex conjugate H*. It is given by

$$Coh_{HH^*}(f) = \left\{ \frac{K_{HH^*}(f)^2 + Q_{HH^*}(f)^2}{\Gamma_{HH}(f)\,\Gamma_{H^*H^*}(f)} \right\}^{1/2} \qquad (2.5)$$

with

$$\Gamma_{H^*H^*}(f) = \Gamma_{HH}(-f)$$

$$K_{HH^*}(f) = \frac{1}{4}(\Gamma_{CC}(f) - \Gamma_{SS}(f))$$

$$Q_{HH^*}(f) = -\frac{1}{2} K_{CS}(f)$$

where K denotes the co-spectrum and Q the quadrature-spectrum. From (2.5) it becomes clear that there are two necessary conditions for the coherence spectrum to be zero, namely equal autospectra for the cosine and the sine coefficient time series and a zero co-spectrum K_{CS}.

As the coherence spectrum the standing wave spectrum is symmetric, i.e. St(f) = St(-f).The remaining variance is assigned to travelling waves:

$$Wa(f) = \Gamma_h(f) - \frac{1}{2} St(f) \qquad (2.6)$$

It also contains irregularly varying components.

The phase spectrum is useful for the standing wavepart only and is defined only if the standing wave variance is nonzero, which is equivalent to $K_{HH^*}(f) \neq 0$ or $Q_{HH^*}(f) = 0$. If this condition is fulfilled the following definition is adequate:

$$Ph_{HH^*} = \begin{cases} \tan^{-1}(-Q_{HH^*}/K_{HH^*}) = \tan^{-1}(2K_{CS}/\Gamma_{CC}-\Gamma_{SS}) & \text{if } \Gamma_{CC} \neq \Gamma_{SS} \text{ and } K_{CS} \neq 0 \\ \pi/2 & \text{if } \Gamma_{CC} = \Gamma_{SS} \text{ and } K_{CS} > 0 \\ -\pi/2 & \text{if } \Gamma_{CC} = \Gamma_{SS} \text{ and } K_{CS} < 0 \\ 0 & \text{if } \Gamma_{CC} > \Gamma_{SS} \text{ and } K_{CS} = 0 \\ \pi & \text{if } \Gamma_{CC} < \Gamma_{SS} \text{ and } K_{CS} = 0 \end{cases} \qquad (2.7)$$

Interpreting this phase spectrum in physical space, an extreme of a standing zonal wavenumber m wave has to be assigned to $P_{HH^*}(f)/2m$. A zonal wavenumber 1 standing sine wave has a phase of 180° but its extreme at 90°. The definition is useful, as is shown by the following examples. If $\Gamma_{CC} = \Gamma_{SS}$, the sine and the cosine are of the same importance and an extreme at 45° is identified. If $\Gamma_{CC} = \Gamma_{SS}$ and $K_{CS} = 0$, no in-phase relationship between C_t and S_t exists and all

standing variance has to be attributed to the dominant pattern, sine or cosine. That is, if $\Gamma_{CC} > \Gamma_{SS}$ the cosine is dominant and we have an extreme at 0°, and if $\Gamma_{CC} < \Gamma_{SS}$ the standing component is given by the sine with $Ph_{HH^*} = \pi$, and has its first extreme at $\pi/2m$.

The question is, whether the decomposition (2.3-4, 6-7) is useful for interpreting a time series of Fourier coefficients generated by bivariate **stochastic** processes. The spectral matrix of the bivariate autoregressive process (1.1) is (Jenkins and Watts, 1968):

$$\Gamma(f) = (I - A^* e^{i2\pi fl})^{-1} \cdot \Gamma_n(f) \cdot (I - A^T e^{-i2\pi f})^{-1} \tag{2.8}$$

In this expression Γ_n is the spectral matrix of the noise vector n_t (see 1.1) and I is the identity matrix. From (2.8), the spectra of real autoregressive processes C_t and S_t of order one are derived to be:

$$\Gamma_{CC}(f) = \frac{\sigma_z^2}{D}(1 + a_{22}^2 - 2a_{22}\cos 2\pi f + b^2 a_{12}^2)$$

$$\Gamma_{SS}(f) = \frac{\sigma_z^2}{D}(a_{21}^2 + b^2(1 + a_{11}^2 - 2a_{11}\cos 2\pi f)) \tag{2.9}$$

$$\Gamma_{CS}(f) = K_{CS}(f) - iQ_{CS}(f)$$

with

$$K_{CS}(f) = \frac{\sigma_z^2}{D}\left\{a_{21}\cos 2\pi f - a_{21}a_{22} + b(a_{12}\cos 2\pi f - a_{11}a_{12})\right\} \tag{2.10}$$

$$Q_{CS}(f) = \frac{\sigma_z^2}{D}\left\{a_{21}\sin 2\pi f - ba_{12}\sin 2\pi f\right\}$$

and

$$D = 1 + a_{11}^2 + a_{22}^2 + 2a_{22}a_{11} + a_{22}^2a_{11}^2 + a_{12}^2a_{21}^2 - 2a_{11}a_{12}a_{21}a_{22} + (a_{22}a_{11} - a_{12}a_{21})2\cos 4\pi f$$

$$- (a_{11} + a_{22} + a_{11}^2a_{22} + a_{11}a_{22}^2 - a_{11}a_{12}a_{21} - a_{22}a_{12}a_{21})\cdot 2\cos 2\pi f \tag{2.11}$$

In the following we consider a number of particular cases of (1.1) and perform the space-time spectral analysis on it. A list of the considered cases is given in Table 1.

Table 1: List of cases considered

no.	name of case	generating process parameters (Sec. 2)		estimation (Sec. 3)			discussed in section
		matrix A	$b = \sigma_z'^2/\sigma_z^2$	specified parameters	fitted process order M	time series length L	
1	standing oscillation and noise	$\begin{matrix} a & 0 \\ 0 & 0 \end{matrix}$	$0 \leqq b$	$a = 0.9$ $b = 1$	1	60	2.1 and 3.1
2	purely noisy behaviour	$\begin{matrix} a & 0 \\ 0 & a \end{matrix}$	1	$a = 0.9$	1	60	2.2 and 3.2
3	travelling waves	$\begin{matrix} \varepsilon & \omega \\ -\omega & \varepsilon \end{matrix}$	$0 \leqq b$	$\varepsilon = 0.8$ $\omega = 0.6$ $b = 1$	1	60	2.3 and 3.3
4	mixed waveforms	$\begin{matrix} a_{11} & a_{12} \\ a_{21} & a_{22} \end{matrix}$	1	$a_{11} = 0.6$ $a_{12} = -0.5$ $a_{21} = 0.4$ $a_{22} = 0.5$ $b = 1$	1 8 1	60 60 300	3.4 3.5 3.6

2.1 Standing oscillations and noise

We consider the case that one of the components C_t or S_t is dominant:

$$a_{11} = a, \quad a_{12} = a_{21} = a_{22} = 0, \quad 0 \le b$$

so that

$$C_t = a\,C_{t-1} + z_t \tag{2.12}$$

$$S_t = z_t'$$

The formalism (2.3-7) establishes

$$\Gamma_h(f) = \frac{B(f)+b}{4}\,\sigma_z^2, \quad Coh_{HH^*}(f) = \frac{|B(f)-b|}{B(f)+b}$$

and

$$St(f) = \frac{|B(f)-b|}{2}\,\sigma_z^2 \quad and \quad Wa(f) = \begin{cases} \frac{b}{2}\sigma_z^2 = \frac{\sigma_z^2}{2} & for\ b < B(f) \\ \frac{B(f)}{2}\sigma_z^2 & for\ b > B(f) \end{cases} \tag{2.13}$$

with

$$B(f) = \frac{1}{1+a^2-2a\cos 2\pi f}$$

B(f) is symmetric with respect to frequency f. Thus, Γ_h (f) and Wa (f) are also symmetric. This is reasonable as (2.12) contain no mutual dependence of S_t and C_t, which could lead to a preference of either westward or eastward travelling waves. Because of the independence of C_t and S_t, the co-spectrum K_{CS} is zero. Generally the coherence Coh_{HH^*} becomes positive and a standing waveform is obtained, the phase of which is that of a sine if $\Gamma_{CC} < \Gamma_{SS}$ and of a cosine if $\Gamma_{CC} > \Gamma_{SS}$. If $\Gamma_{CC} = \Gamma_{SS}$ the phase is undefined, since the standing wave amplitude is zero.

In the particular case b = 0, the sine coefficient, S_t, is constantly zero and the cosine coefficient, C_t, is given by an autoregressive process of order one. Since one component is fixed, the bivariate random variable (C_t, S_t) is restricted to a

one-dimensional subspace, i.e. the phase is fixed. Thus, this process ought to be identified as a purely standing wave. Insertion of $b = 0$ in (2.13) leads actually to $St(f) = \Gamma_h(f)$, $Ph_{HH^*}(f) = 0$, and $Wa(f) = 0$.

2.2 Purely noisy behavior

Now the sine and cosine Fourier coefficients C_t and S_t are considered, which are generated by two independent autoregressive processes of the first order. In particular, we assume

$$a_{11} = a_{22} = a\,, \qquad a_{12} = a_{21} = 0, \qquad b = 1$$

The time evolution of the sine and the cosine coefficients is described by

$$C_t = a\,C_{t-1} + z_t \tag{2.14}$$

$$S_t = a\,S_{t-1} + z_t'$$

Because of the lack of any cross-relationship between S_t and C_t the amplitude and phase of the two-dimensional (C_t, S_t) vector vary irregularly : Thus, the analysis should identify a zero standing component and distribute all variance equally to eastward and to westward propagating disturbances. Indeed, this is the scheme's result:

$$\Gamma_h(f) = \frac{B'(f)}{2}\,\sigma_z^2 \qquad Coh_{HH^*}(f) = \frac{1-b}{1+b} = 0 \tag{2.15}$$

therefore $\qquad St(f) = 0 \qquad Wa(f) = \dfrac{B'(f)}{2}\,\sigma_z^2$

with $$B'(f) = \frac{1 + a^2 - 2a\cos 2\pi f}{1 + 4a^2 + a^4 - 4(a + a^3)\cos 2\pi f + 2a^2\cos 4\pi f}$$

Because of zero off-diagonal elements of A, the co-spectrum K_{CS} and thus the quad-spectrum Q_{HH^*} are zero (2.10 and 2.5) independently of the value of b. If b = 1, the cosine and sine autospectra are identical and the co-spectrum K_{HH^*} vanishes, leading to the useful result of an undefined phase.

If the variance ratio b is not equal to 1, the co-spectrum K_{HH^*} becomes positive ($b < 1$) or negative ($b > 1$) and nonzero coherence Coh_{HH^*} is obtained leading to a standing component, given by the cosine ($b < 1$) or the sine ($b > 1$) pattern.

2.3 Travelling waves

If the coefficients of the matrix A fulfil the condition

$$a_{11} = a_{22} = \varepsilon > 0, \qquad a_{12} = -a_{21} = \omega \tag{2.16}$$

the eigenfunctions of the matrix A reflect a damped oscillation with frequency $f_o = tan^{-1}\ (\omega/\varepsilon)\ /\ 2\pi$. For positive (negative) coefficients ω the wave moves westward (eastward).

The frequency-wavenumber spectra are given by:

$$\Gamma_h(f) = \frac{B''(f)}{4}\,\sigma_z^2$$

$$Coh_{HH^*}(f) = \left|\frac{1-b}{1+b}\right| \left\{\frac{(E-\omega^2)^2 + 4(\omega\cos 2\pi f - \omega\varepsilon)^2}{(E+\omega^2)^2 - 4(-\omega\sin 2\pi f)^2}\right\}^{1/2} \tag{2.17}$$

$$Ph_{HH^*}(f) = \begin{cases} tan^{-1}\left(\dfrac{-\omega\cos 2\pi f + \omega\varepsilon}{E-\omega^2}\right) & if\ b=1 \\ undefined & if\ b=1 \end{cases}$$

$$with \qquad B''(f) = \frac{(1+b)(E+\omega^2+2\,\omega\sin 2\pi f)}{D} \qquad and \qquad E = 1+\varepsilon^2-2\varepsilon\cos 2\pi f$$

and D given by (2.11).

For $\omega > 0$ and $f \geqq 0$, we find $\Gamma_h(f) \leqq \Gamma_h(-f)$. That is for $\omega > 0$ the westward travelling waves dominate the eastward travelling waves. For $\omega < 0$, most of the variance is assigned to eastward travelling waves. For a process with a variance ratio b = 1, the coherence spectrum is zero everywhere and the space time spectral analysis correctly identifies a purely travelling wave.

If the coefficients a_{ij} do not fulfill the condition (2.14) exactly or the variance ratio b is smaller than one, the real time series C_t and S_t are correlated and have different autospectra Γ_{CC} and Γ_{SS}. Therefore a non-zero coherence and phase spectrum is obtained and a standing wave is identified.

A basic condition that a fully statisfactory scheme to separate travelling and standing waves should fulfill is that $St(f) \geqq 0$ and $Wa(f) \geqq 0$. The standing wave spectrum is nonnegative according to (2.4). $Wa(f) \geqq 0$ is not automatically fulfilled, but equivalent to the nontrivial condition (see(2.6)):

$$\frac{St(f)}{2} \leq \Gamma_h(f) \tag{2.18}$$

For some combinations of parameters (2.18) is violated. To demonstrate this, (2.18) is rewritten using (2.3-5):

$$(\Gamma_{CC}-\Gamma_{SS})^2 + K_{CS}^2 \leq (\Gamma_{CC}+\Gamma_{SS}-2Q_{CS})^2 \tag{2.19}$$

A variance ratio b clearly different from 1 leads to large differences of Γ_{CC}-Γ_{SS}, and large ω numbers to large co and quadrature-spectra K_{CS} and Q_{CS}, which are both proportional to ω (2.10). One example represents the combination of the parameters $b = 0.1$, $\varepsilon = 0.5$ and $\omega = 0.8$. It leads to negative spectral densities of the travelling waves at the negative maximum frequency, $f_0 = -0.17$, accounting for 5% of $\Gamma_h(f_0)$.

3.Unknown stochastic processes

For the estimation of the spectral matrix, two approaches are generally used:

* estimation of the cross-covariance function at as many lags as possible and calculation of the spectrum as a discrete Fourier transformation of the estimated cross-covariance function.
* fitting a bivariate autoregressive process to the data and the use of the spectral matrix of that fitted autoregressive process (Maximum Entropy Method (MEM)).

We use the MEM-approach, which is quite economic and asymptotically unbiased and yields a fine spectral resolution for a short time series (Hayashi, 1981).

We want to find out to what extent the potential merits of the procedure, as described in Section 2, are affected by the necessity to estimate unknown parameters. For this purpose, we perform a number of Monte Carlo experiments, in which we consider finite time series which are generated by means of process (1.1) with prescribed matrices A.

Processes (1.1) which were found in Section 2 to be connected with standing wave and noise, purely noisy behavior, purely travelling wave and mixed waveform are considered (Table 1). For each example, an ensemble of 50 independent time series of record length L is generated. Each of these 50 time series is fitted to an autoregressive process of order M. In that way, 50 independent spectra are formed. Sample means and standard deviations of the spectral density are calculated. That is, the mean spectra are the mean of 50 sample spectra and not the spectra of the averaged spectral matrix.In the diagrams the estimated mean spectra are plotted as light lines and the theoretical spectra,which were found in Section 2, as heavy lines. To indicate the inter-sample variability, a vertical line centered at the mean with a length equal to twice the standard deviation of the estimate is added. Thus, about 70% of all of the samples are inside the hatched band.

In Section 3.1 to 3.4 the order M of the fitting process is set to 1, which is the order of the generating process, and the time series length is L = 60. In Section 3.5, the sensitivity of the frequency wavenumber analysis to overestimating the correct order by M is tested by considering one example with M = 8. The

generating process order M = 1 is used in Section 3.5, where the effect of an increased time series length, L = 300, is studied.

3.1 Standing oscillation and noise

We study the case "standing wave plus noise" (case 1 in Table 1) by considering a Monte Carlo simulation using the parameters $a = 0.9$, $b = 1$ and $M = 1$. The frequency-wavenumber spectrum is well analyzed (not shown).

The coherence spectrum is weakly overestimated, as is demonstrated by Figure 1A. The heavy line shows the true coherence spectrum (2.13). The vertical hatching indicates the 70% band centered at the mean estimated coherence spectrum containing about 70% of all individual estimated spectra. The dotted area refers to estimates with $M = 8$ and will be discussed in Section 3.5. The overestimation of the coherence spectrum is largest where the true spectrum is close to zero. That is reasonable, and will be found in the other cases considered in the next subsections, because coherence squared can be thought of as a correlation coefficient squared. That is, if the true correlation at some frequency is zero, the estimated correlation squared will always be positive.

To indicate the intersample variability of the coherence and phase estimation, we show the 50 normalized estimated co- and quadspectra K_{HH^*} and Q_{HH^*} at the maximum frequency $f_0 = 0$ in Figure 2. Each estimation is given by a dot. The length of a vector pointing from the origin to the dots is the coherence, and the angle spanned by the horizontal axis and the vector is the phase. The true values $Coh_{HH^*}(f_0) = 1$ and $Ph_{HH^*}(f_0) = 0$ are depicted by an open circle. Clearly, all estimates are in a close neighbourhood of the true point. For higher frequencies the estimates of the phase becomes less reliable (not shown).

Fig. 1.: Coherence spectra (Coh_{HH^*}) from time series with length L = 60. Heavy solid line: theoretical coherence spectrum. 70% of all estimated sample spectra for autoregressive process order M = 1(8) in the vertically hatched (dotted) band.

(A) standing wave superimposed with noise, a = 0.9, b = 1 (case 1 of Table 1)

(B) red noise, a = 0.9, b = 1 (case 2 of Table 1)

(C) westward travelling without a standing component, $\varepsilon = 0.8$, and $\omega = 0.6$, b = 1(case 3 of Table 1).

(D) eastward travelling wave with a small standing wavepart (case 4 of Table 1)

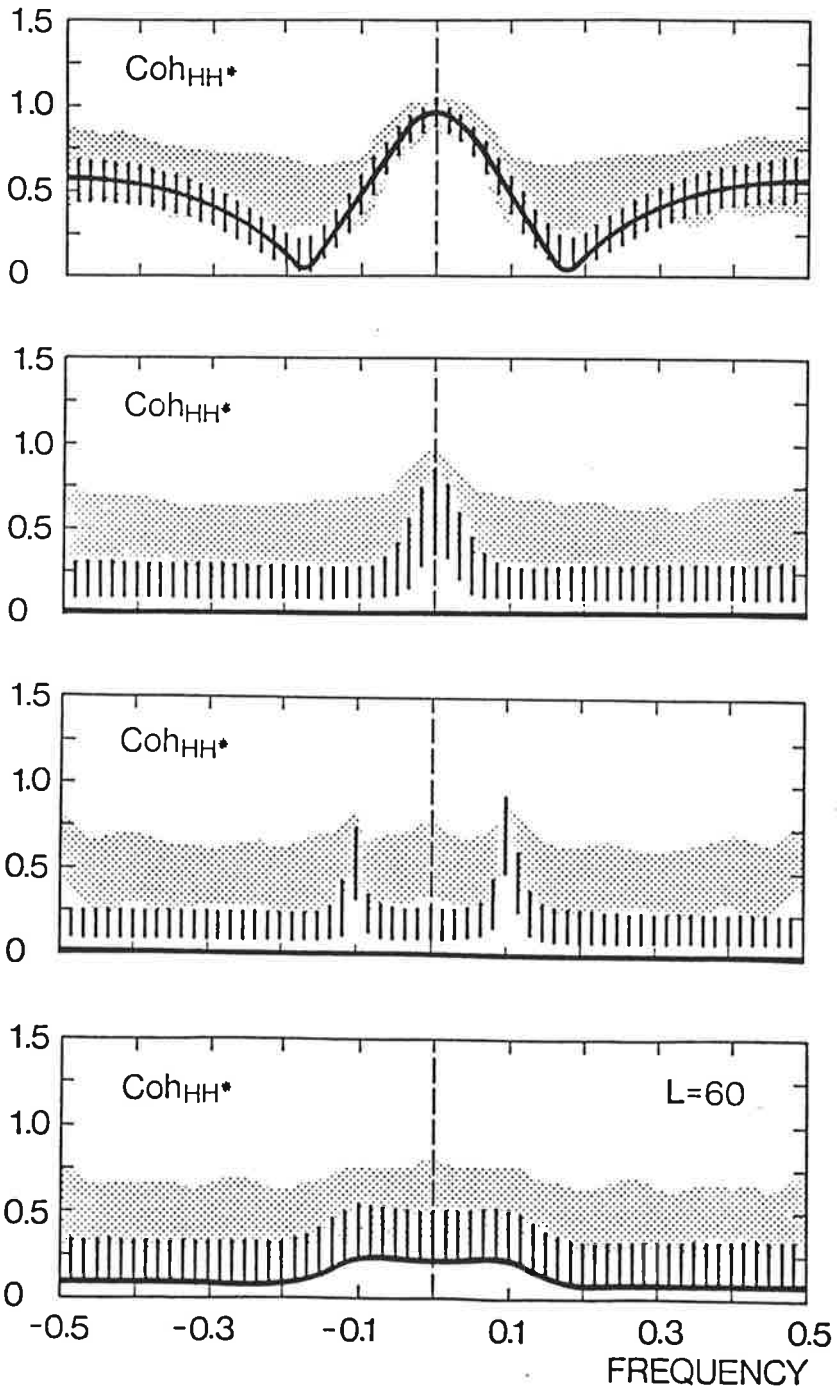

Fig. 2: Standing wave and noise (case 1 of Table 1; see Section 3.1): Sample variability of the 50 estimated co-and quadrature-spectra K_{HH^*} and Q_{HH^*} normalized by $(\Gamma_{HH}\Gamma_{H^*H^*})^{1/2}$ at the maximum frequency f_0. Each estimation is given by a dot. The length of a vector pointing from the origin to the dots is the coherence, and the angle spanned by the horizontal axis and the vector is the phase. The true values $Coh_{HH^*}(f_0)$ and $Ph_{HH^*}(f_0)$ are depicted by an open circle.

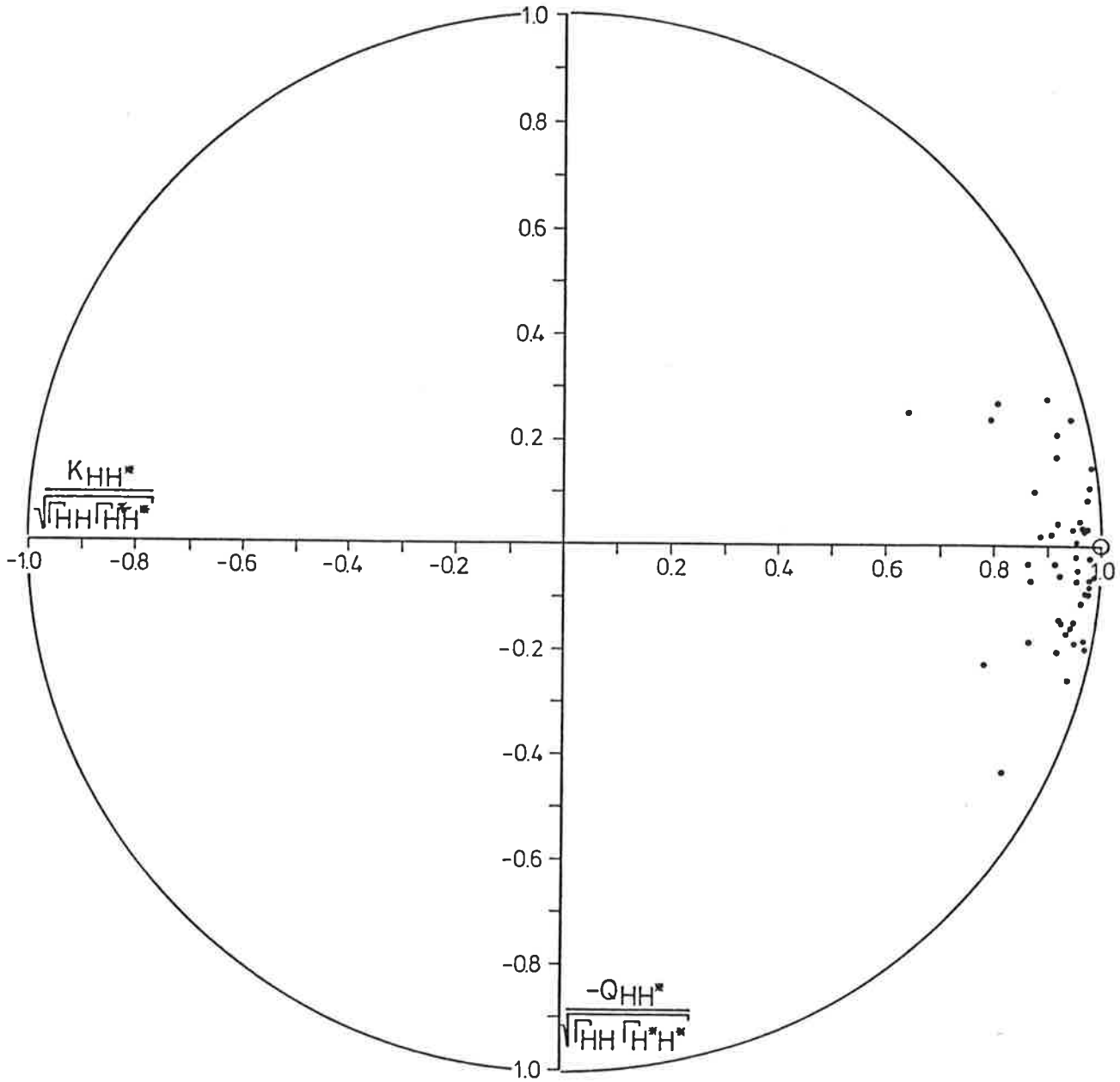

3.2 Purely noisy behavior

Case 2 in Table 1, "purely noisy behavior", is considered by means of a Monte Carlo example with a = 0 9, b = 1 and M = 1 (Fig.3). Not only the mean but most of the individual estimated frequency wavenumber spectra appear symmetric, which is in accordance with the true spectrum of this case (see (2.15)). The low-frequency Γ_h-variance is considerably underestimated. This might be related to the general experience that the estimated parameters of an autoregressive process tend to stay away from the boundary of the region of stationarity and the parameter used here, a = 0.9, is quite close to the boundary at a = 1.

After having found step (c), mentioned in the Introduction, behaving relatively well, we get unfavorable results for step (d), the separation into travelling and standing wave variance: As the true coherence spectrum Coh_{HH^*} is zero everywhere (see (2.15)) we might expect the estimated coherence to be overestimated everywhere. That is indeed the case and mean coherencies of as much as 60% are identified erroneously at low frequencies (Fig. 1B). As a consequence the analysed system is incorrectly described as being composed totally of non-standing waves. In fact, a significant standing component is filtered out (Fig.3).

In Section 2.2 we found the phase to be undefined. A plot, similar to Fig 2 of the 50 coherencies and phases at the maximum frequency $f_0 = 0$ derived from the 50 Monte Carlo experiments reveals that there is no systematic error in the phase estimate (not shown): The distribution of the dots is uniform with respect to the angle. However, if just one sample is available one has to expect large errors. The variability is nearly the same for all frequencies.

Fig. 3.: Frequency-wavenumber spectra (Γ_h), the spectra of standing (St) and travelling (Wa) wavepart of red noise (a = 0.9) discussed in Section 2.2 and 3.2.(case 2 in Table 1). Time series length L = 60 and order of the fitted process M = 1.
Heavy solid line: theoretical spectrum
Light solid line: mean estimated spectrum
The vertically hatched band is centered at the mean estimate and contains roughly 70% of all estimated sample spectra.

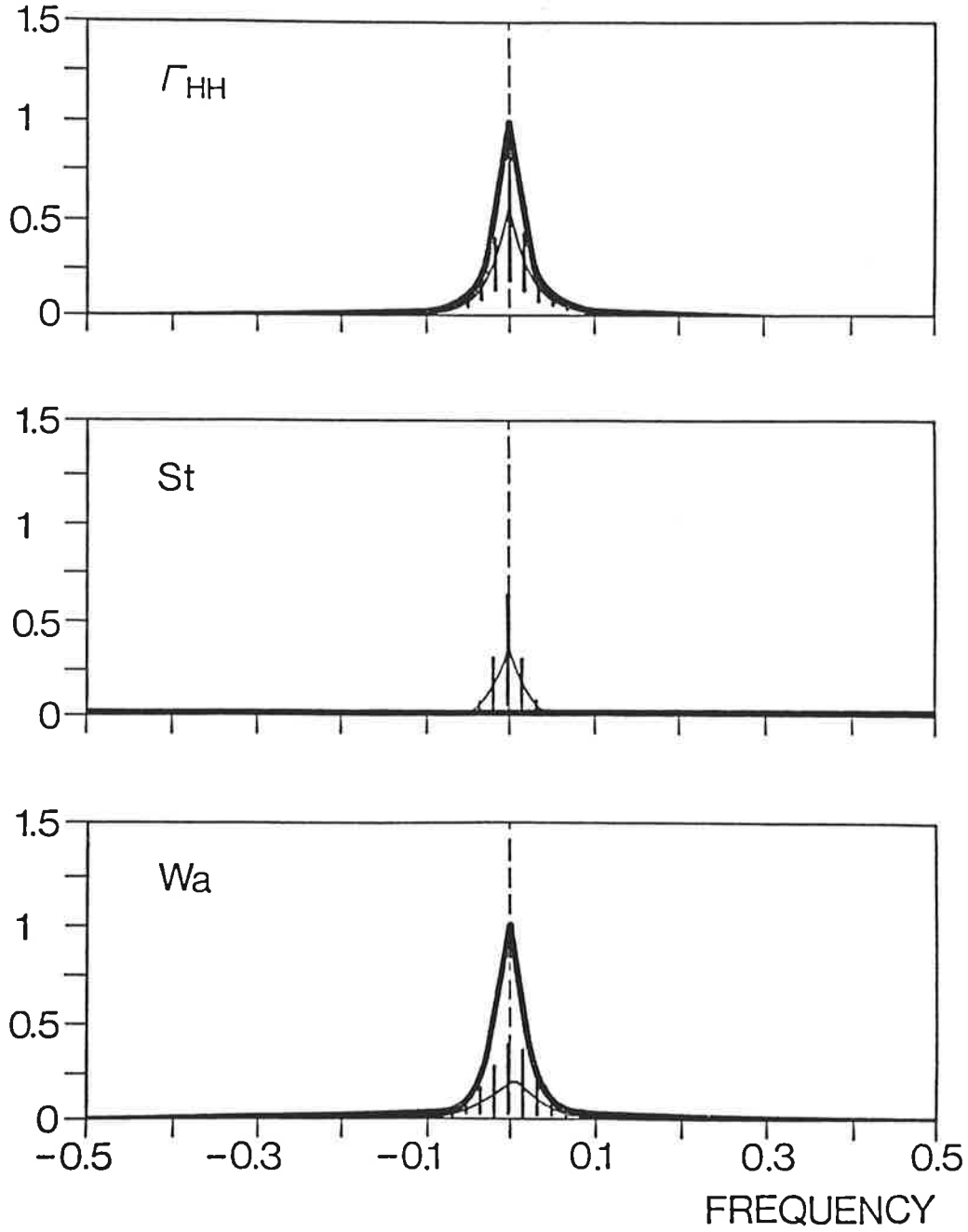

3.3 Purely travelling waves

The Monte Carlo example used to study case 3 of Table 1, "purely travelling waves", is run with the parameters $\varepsilon = 0.8$, $\omega = 0.6$ and $b = 1$ (no diagrams shown). Similar to Section 3.2, the shape of the frequency wavenumber spectrum is interpreted correctly, even in most of the individual cases: Most of the variance is attributed to westward moving waves, and the maximum frequency of the ensemble mean spectrum has the right location, $f_0 = \tan^{-1}(\omega/\varepsilon)2\pi$ (see Section 2.3). Also similar to Section 3.2, the general level of the variance is too low and partly underestimated by as much as 50%.

Because of $b = 1$, the true coherence spectrum is zero everywhere (see (2.17)). Not unexpectedly the coherence estimator is positively biased (Fig. 1C) and the analysis generates an artificial standing wave component, the phase of which is uniformly distributed.

3.4 Mixed waveforms

As a final example case 4 of Table 1 is considered using $a_{11} = 0.6$, $a_{22} = 0.5$, $a_{12} = -0.5$ and $a_{21} = 0.4$, $b = 1$ and $M = 1$. Calculating the theoretical spectrum, we find that most of the variance is due to an eastward travelling wave and a minor portion is contributed by a standing wave (Fig.4). The travelling wave's maximum frequency is $f_0 = -0.12$, and that of the standing eastward travelling wave at $f_0 = \pm 0.12$. The frequency wavenumber spectrum is very well estimated (Fig.4). As opposed to the results from the preceding subsections, the quantitative separation into standing and travelling waves is not too bad (Fig.4), because of a coherence spectrum only weakly overestimated (Fig. 1D).

Coherences and phases of the true spectrum (open circles) and the 50 estimates (dots) at the maximum frequency $f_0 = -0.12$ are shown in Figure 5. The theoretical values ($Coh_{HH^*}(f_0) = 0.2$, $Ph_{HH^*}(f_0) = 22°$) are given by the open circle. The estimates vary considerably, but there is a preferred area characterized by a line linking the origin and the true value.

Fig. 4.: Frequency-wavenumber spectrum ($\Gamma_{..}$),the spectra of standing (St) and travelling (Wa) wavepart of an eastward travelling wave with a small standing part discussed in section 3.4 (case 4 in Table 1). Time series length L = 60 and order of the fitted process M = 1. Symbols: see Fig. 3.

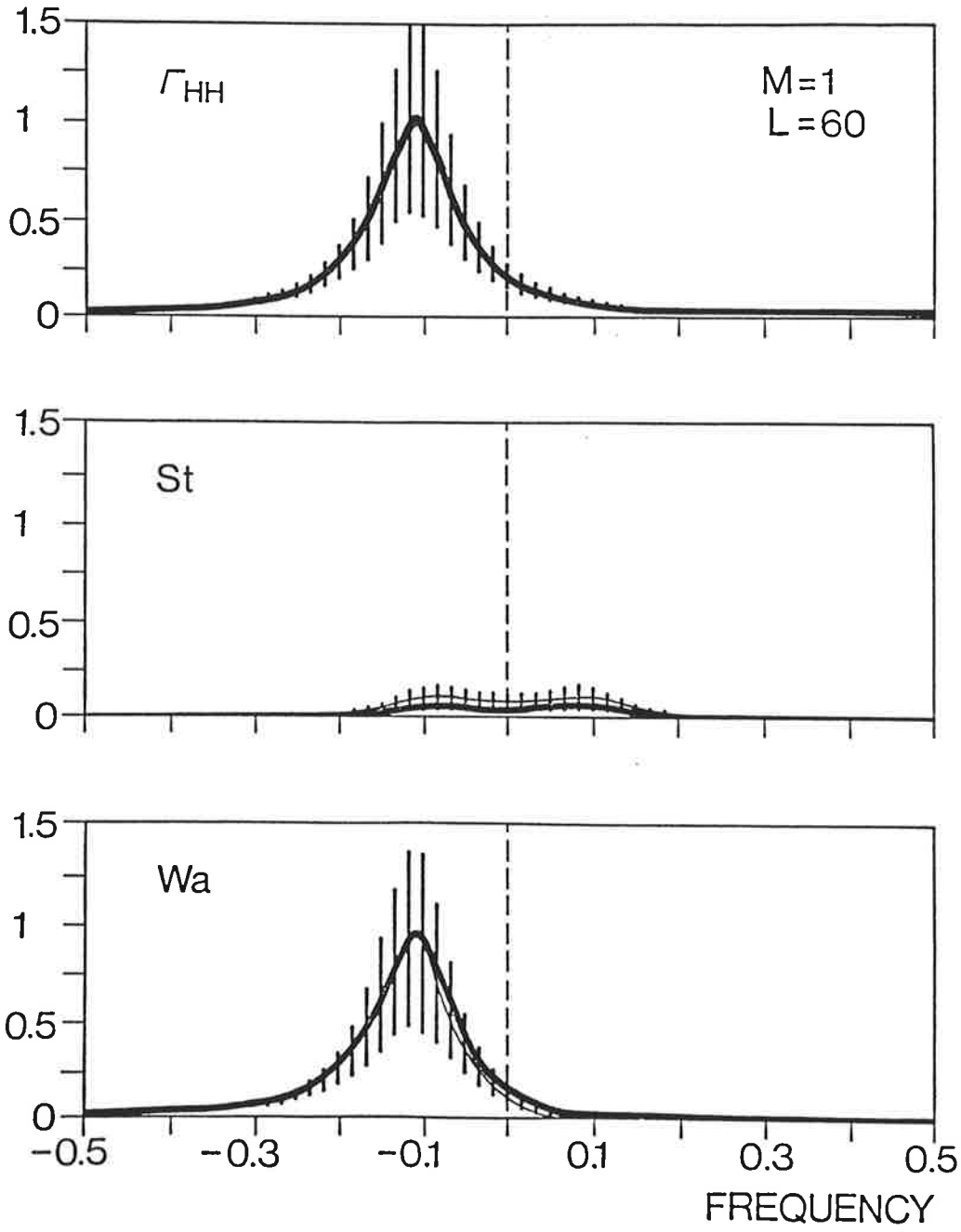

Fig. 5.: Eastward travelling wave with a small standing wavepart (case 4 of Table 1; see Section 3.4):
Sample variability of the 50 estimated co-and quadrature-spectra K_{HH^*} and Q_{HH^*} normalized by $(\Gamma_{HH}\Gamma_{H^*H^*})^{1/2}$ at the maximum frequency f_0. Each estimation is given by a dot. The length of a vector pointing from the origin to the dots is the coherence, and the angle spanned by the horizontal axis and the vector is the phase. The true values $Coh_{HH^*}(f_0)$ and $Ph_{HH^*}(f_0)$ are depicted by an open circle.

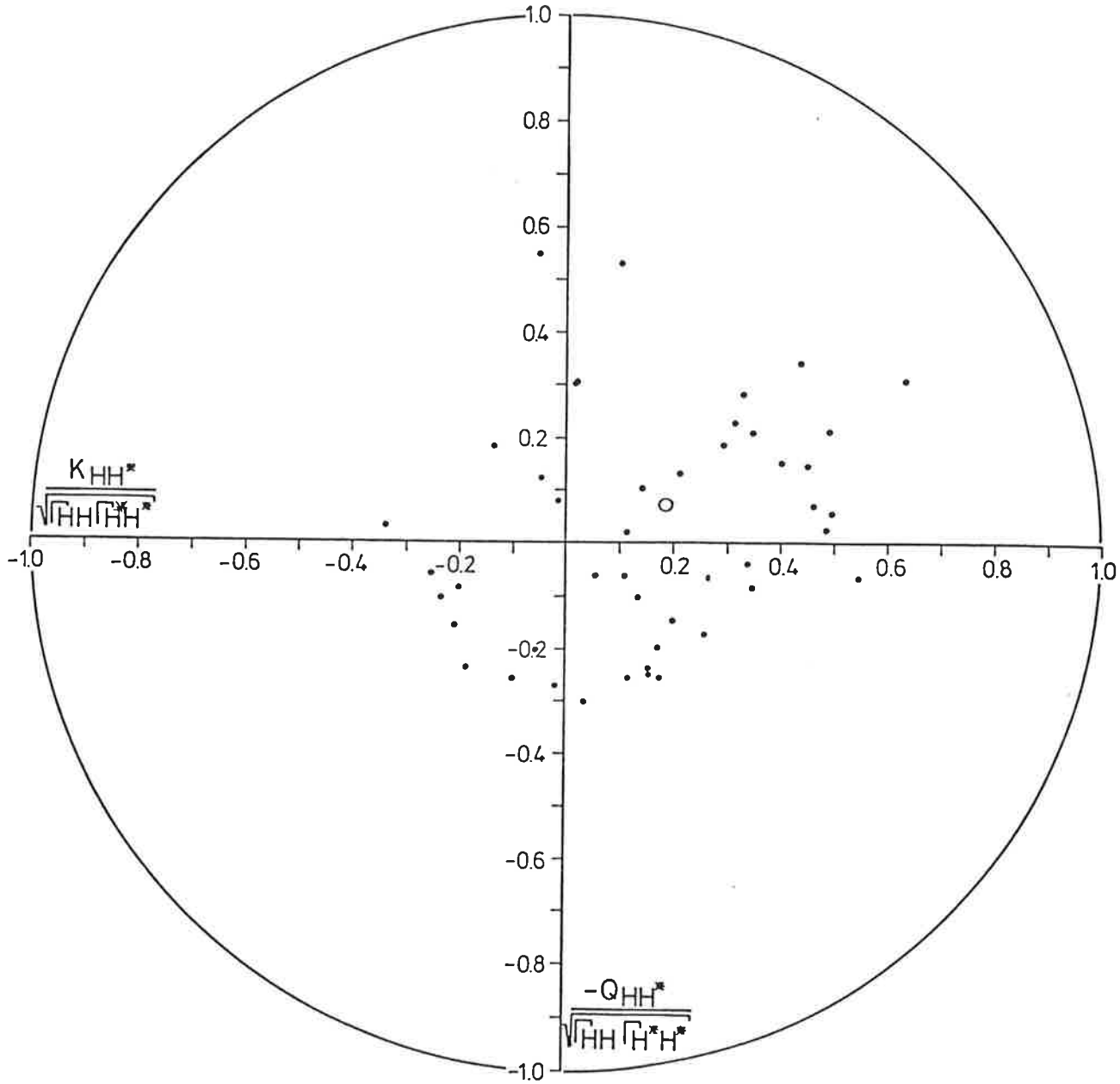

Fig. 6.: Eastward travelling wave with a small standing part (case 4 in Table 1): Sample variability of the 50 estimated co- and quadrature-spectra K_{HH^*} and Q_{HH^*} normalized by $(\Gamma_{HH}\Gamma_{HH^*})^{1/2}$ at the maximum frequency $f_0 = -0.12$ (same as Fig.5).
Crosses (solid dots) refer to estimates using L = 60 samples and M = 8 fitting processes (L = 300, M = 1).
The open dot is the theoretical value.

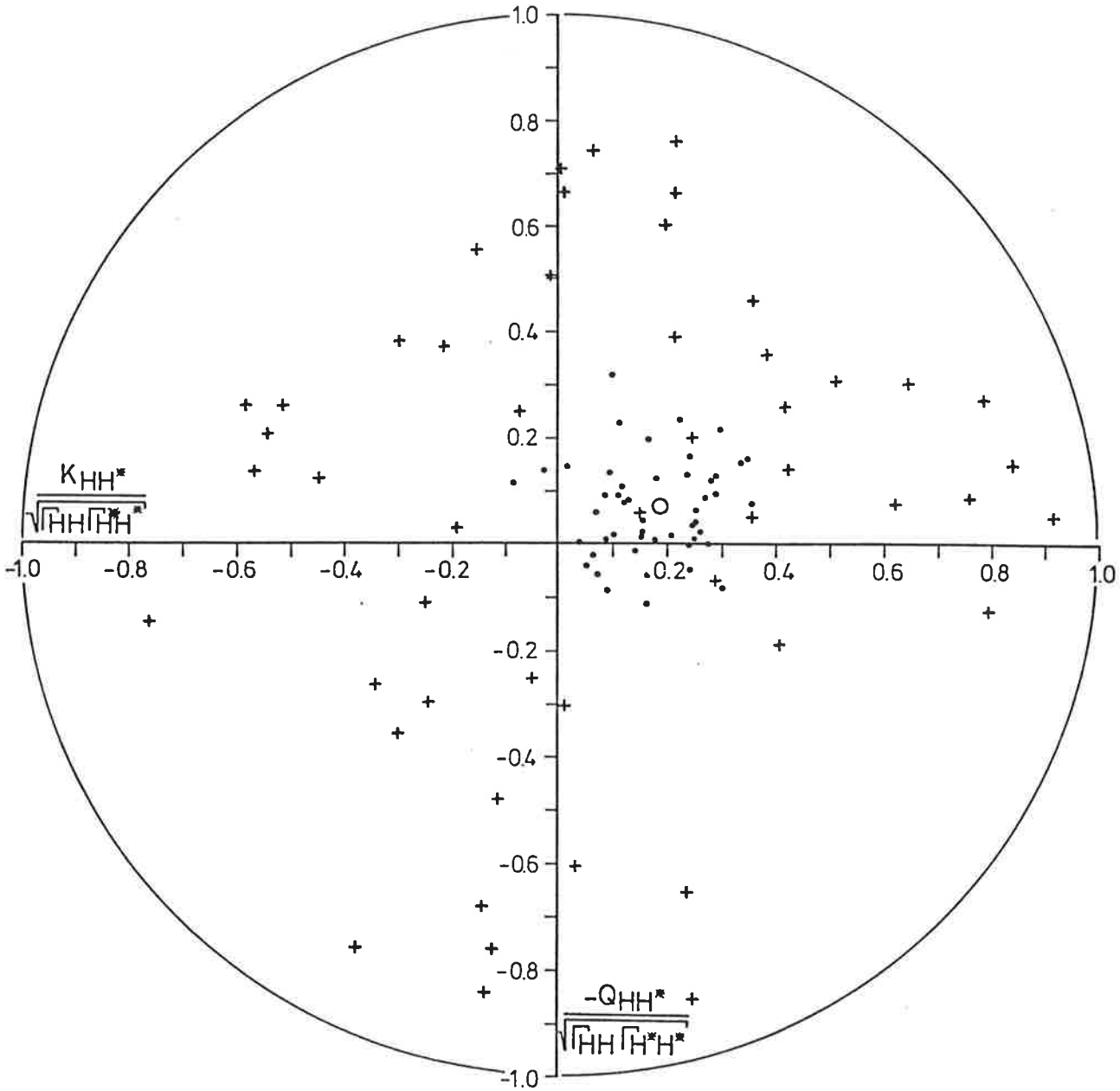

3.5 Sensitivity to process order M

In practice, the appropriate process fitting order M is unknown. Thus, one will generally overestimate this order, since the algorithms (Akaike and Bayesian information criterions) given in the literature to select the "correct order" are only of limited reliability.

To study the effect of overestimating the correct order, the "mixed waveform" example (case 4 of Table 1) discussed in Section 3.4 is considered again with a fitting process order M = 8. The frequency wavenumber spectrum (Γ_h) estimator is unbiased but its variance (not shown) is increased if compared with the Monte Carlo results from the M = 1 analyses in Section 3.4. The bias of the coherency estimate is about 50% at all frequencies (see dotted band in Figure 1D) and clearly worse than the estimate using the correct order M = 1 (dashed band in Figure 1D). The intersample variability of coherence and phase, which is shown at the maximum frequency f_0 = -0.12 in Figure 6 (crosses), is considerably increased if M = 8 instead of the correct M = 1 (Fig.5) is used.

This unfavorable effect of an increased expected error of the coherence spectrum, and thus of the variance of standing waves, is common to all examples of Table 1. As a demonstration of this, the M = 8 estimates of the coherence are added to the results obtained with the correct order M = 1 in Figure 1 as dotted band.

3.6 Sensitivity to time series length L and ensemble size

It is generally accepted that the ME spectra estimator is consistent, i.e. that an increase of record length L causes a reduction of sample variance and bias. This turns out to be valid for the frequency wavenumber analysis as well. We demonstrate this by examining once again the "mixed waveform" case 4 of Table 1. Here, the estimations are based on time series of lengths $L = 300$, in contrast to Section 3.4, where $L = 60$ was used. The order of the fitting process is chosen to be the correct one, $M = 1$. Not only the mean frequency wavenumber estimate but also the mean estimated coherence spectrum coincide well with the true spectrum (not shown). The intersample variability is significantly decreased, if compared with the $L = 60$ case. This is clearly demonstrated by the phase/coherence diagram at the maximum frequency f_0 shown in Fig.6 by solid dots.

Up to this point we have considered the characteristics of spectral estimates when only one single time series is given. If the total data given may be subdivided in a number of chunks, the coherence could be obtained from the averaged auto-and cross spectra derived from the chunks. If this method is used, the bias of the coherence estimate does in fact reduce, and a trustworthy separation into standing and travelling waves is gained (not shown).

Conclusion

We have examined the utility of space-time spectral analysis for inferring the characteristics of wavy components in stochastic time series.

For stochastic processes with known spectra, the space-time spectral analysis yields a reasonable decomposition in all but one of the examples considered. It fails when used to analyse a damped oscillation forced with nonisotropic white noise. In this case the scheme's working assumption of the standing and travelling waves being statistical independent is significantly violated leading to travelling wave variance spectra, which is partly negative.

If only finite time series are available, estimated spectra have to be inserted into the formulae. We find the frequency-wavenumber spectra reasonably estimated although the (total) variance was sometimes underestimated. The results indicate that the separation into east- and westward moving components is adequate. However, the separation into standing and travelling components by means of the estimated coherence spectrum turns out to be critical: The coherence spectrum is often greatly overestimated resulting in a corresponding positive bias of the standing wave variance. The overestimation of coherence is most severe if the true coherence is close to zero. Since coherence may be seen as a correlation squared, this deficiency appears unavoidable.

This problem with bias is most pronounced when only one short time series is available and the order of the fitted autoregressive process is overfitted. In that case the analysis of standing and travelling waves becomes useless. For longer time series or greater ensembles of short time series, the results gradually improve. If, for example, midlatitude winter 500 mb along a certain latitude were to be considered, it would not be useful to calculate the standing and travelling wave variance for just one winter. However, if a multiyear time series or data from a number of winters were available, the ensemble averaged information derived from space-time spectral analysis would appear to be useful.

Figure captions

Fig. 1.: Coherence spectra (Coh_{HH^*}) from time series with length L = 60. Heavy solid line: theoretical coherence spectrum. 70% of all estimated sample spectra for autoregressive process order M = 1(8) in the vertically hatched (dotted) band.
(A) standing wave superimposed with noise, a = 0.9, b = 1 (case 1 of Table 1)
(B) red noise, a = 0.9, b = 1 (case 2 of Table 1)
(C) westward travelling without a standing component, $\varepsilon = 0.8$, and $\omega = 0.6$, b = 1(case 3 of Table 1).
(D) eastward travelling wave with a small standing wavepart (case 4 of Table 1)

Fig. 2: Standing wave and noise (case 1 of Table 1; see Section 3.1):
Sample variability of the 50 estimated co-and quadrature-spectra K_{HH^*} and Q_{HH^*} normalized by $(\Gamma_{HH}\Gamma_{H^*H^*})^{1/2}$ at the maximum frequency f_0. Each estimation is given by a dot. The length of a vector pointing from the origin to the dots is the coherence, and the angle spanned by the horizontal axis and the vector is the phase. The true values $Coh_{HH^*}(f_0)$ and $Ph_{HH^*}(f_0)$ are depicted by an open circle.

Fig. 3.: Frequency-wavenumber spectra (Γ_h), the spectra of standing (St) and travelling (Wa) wavepart of red noise (a = 0.9) discussed in Section 2.2 and 3.2.(case 2 in Table 1). Time series length L = 60 and order of the fitted process M = 1.
Heavy solid line: theoretical spectrum
Light solid line: mean estimated spectrum
The vertically hatched band is centered at the mean estimate and contains roughly 70% of all estimated sample spectra

Fig. 4.: Frequency-wavenumber spectrum (Γ_h),the spectra of standing (St) and travelling (Wa) wavepart of an eastward travelling wave with a small standing part discussed in section 3.4 (case 4 in Table 1). Time series length L = 60 and order of the fitted process M = 1. Symbols: see Fig. 3.

Fig. 5.: Eastward travelling wave with a small standing wavepart (case 4 of Table 1; see Section 3.4):
Sample variability of the 50 estimated co-and quadrature-spectra K_{HH^*} and Q_{HH^*} normalized by $(\Gamma_{HH}\Gamma_{H^*H^*})^{1/2}$ at the maximum frequency f_0. Each estimation is given by a dot. The length of a vector pointing from the origin to the dots is the coherence, and the angle spanned by the horizontal axis and the vector is the phase. The true values $Coh_{HH^*}(f_0)$ and $Ph_{HH^*}(f_0)$ are depicted by an open circle.

Fig. 6.: Eastward travelling wave with a small standing part (case 4 in Table 1):
Sample variability of the 50 estimated co- and quadrature-spectra K_{HH^*} and Q_{HH^*} normalized by $(\Gamma_{HH}\Gamma_{HH^*})^{1/2}$ at the maximum frequency $f_0 = -0.12$ (same as Fig.5).
Crosses (solid dots) refer to estimates using $L = 60$ samples and $M = 8$ fitting processes ($L = 300$, $M = 1$).
The open dot is the theoretical value.

References

Deland, R.J., 1964: Travelling planetary waves. Tellus, 16, 271 - 273.

Hayashi, Y., 1971: A generalized method of resolving disturbances into progressive and retroprogressive waves by space Fourier and time cross-spectral analysis. J. Meteor. Soc. Japan, 49, 125 - 128.

Hayashi, Y., 1973: A method of analyzing transient waves by space-time cross spectra. J. Appl. Meteor., 12, 404 - 408.

Hayashi, Y., 1977: On the coherence between progressive and retrogressive waves and a partition of space-time power spectra into standing and travelling parts. J. Appl. Meteor., 16, 368 - 373.

Hayashi, Y., 1981: Space-time spectral analysis using the maximum entropy method. J. Meteor.Soc. Japan, 59, 620 - 624.

Hayashi, Y., 1982: Space-time spectral analysis and its applications to atmospheric waves. J. Meteor. Soc. Japan, 60, 156 - 171.

Jenkins, G.M. and D.G. Watts, 1968: Spectral analysis and its applications. Holden Day, San Francisco, California.

Kao, S.K., 1968: Governing equations and spectra for atmospheric motion and transports in frequency-wavenumber space. J. Atmos. Sci., 25, 32 - 38.

Kao, S.K., 1970: Wavenumber-frequency spectra of temperature in the free atmosphere. J. Atmos. Sci., 27, 1000-1007.